International Journal of Mechanical and Materials Engineering (IJMME), Vol. 5 (2010), No.2, 276-281

MODELLING OF THE DYNAMICS OF A DROPLET USING THE LATTICE BOLTZMANN METHOD

C.S.N. Azwadi[1] and M.R.M. Zin[2]
[1]Faculty of Mechanical Engineering, Universiti Teknologi Malaysia, 81310 UTM Skudai, Johor, Malaysia
[1]Faculty of Mechanical Engineering, Universiti Teknikal Malaysia Melaka, Melaka, Malaysia
Email:azwadi@fkm.utm.my

Received 13 October 2009, Accepted 3 June 2010

ABSTRACT

This paper deals with the simulation of single-component two-phase fluid flows in two dimensions using the lattice Boltzmann method. We start by describing the theory of the free energy multiphase lattice Boltzmann model. After showing how the formulation of the particles interaction fits into the framework of the lattice Boltzmann simulation, numerical results of a droplet falling and spreading are presented to highlight the capability of this approach to simulate the dynamics of a droplet.

Keywords: Lattice Boltzmann method, Landau free energy, multiphase, droplet dynamics

1. INTRODUCTION

Conventional methods for simulating two- phase flow consist of numerical integration of the Navier-Stokes equations and molecular dynamics simulations. These techniques are extremely computationally intensive and particularly difficult to implement in a random geometry. In recent years, the lattice Boltzmann method (LBM) has become an established numerical scheme for simulating multi-phase fluid flows (Shan and Chen, 1993, Swift et al, 1995, Azwadi et al, 2007, Hasanuzzaman et al. 2007, 2009). The key idea behind the LBM is to recover the correct macroscopic motion of the fluid by incorporating the complicated physics of the problem into simplified microscopic models or mesoscopic kinetic equations.

There are three types of multiphase lattice Boltzmann models that are frequently used. The first type is the so-called coloured model for immiscible two-phase flow proposed by Gunstensen et al. (1991) and based on the original lattice gas model by Rothman and Keller (1988). Gunstensen et al. used coloured particles to distinguish between different phases. However, the coloured model has some limitations in that the model is not rigorously based upon thermodynamics, so it is difficult to incorporate macroscopic physics into the model. The second type of LB approach to model multi-component fluids was derived by Shan and Chen (1993) and later known as the SC model. In the SC model, a non-local interaction force between particles at neighbouring lattice sites is introduced. The net momentum, modified by interparticle forces, is not conserved by the collision operator at each local lattice node, yet the global momentum conservation of the system is exactly satisfied when boundary effects are excluded. The main drawback of the SC model is that it is not well established thermodynamically. One cannot introduce temperature, since the existence of any energy-like quantity is not known. The third type of LB model for multiphase flow is based on the free-energy (FE) approach, developed by Swift et al. (1995), who imposed an additional constraint on the equilibrium distribution functions. This free-energy approach provides more realistic contact angles and fluid density profiles near the vicinity of an impenetrable wall which cannot be easily obtained by other LBM schemes. The FE model conserves mass and momentum locally and globally, and it is formulated to account for equilibrium thermodynamics of nonideal fluids, allowing for the introduction of a well-defined temperature and thermodynamics.

In the present study, we applied the proposed Gallilean invariance free energy approach (Briant et al., 2002, Azwadi et al, 2007) to simulate droplet dynamics on a horizontal flat plate at various contact angles. The simulations were carried out under gravitational and non-gravitational conditions. The obtained results were compared with the available results in literature. Subsequently, the phenomenon of a droplet falling from a top flat wall was examined and quantitatively compared with the benchmark solution.

2. NUMERICAL METHOD

The starting points for the lattice Boltzmann simulations is the evolution equation, discrete in space and time, for a set of distribution functions f. If a two-dimensional nine-velocity model (D2Q9) is used, then the evolution equation for a given f takes the following form (Azwadi and Idris, 2010):

$$f_i\left(\mathbf{x}+\mathbf{e}_i\Delta t, t+\Delta t\right)-f_i\left(\mathbf{x}, t\right)=\frac{1}{\tau}\left[f_i-f_i^{eq}\right] \quad (1)$$

where Δt is the time step, $\mathbf{e}$ is the particle's velocity, τ is the relaxation time for the collision and $i = 0,1,\ldots,8$. It may be noted that the term on the right hand side of Equation (1) is the collision term where the Bhatnagar-Gross-Krook approximation has been applied (Bhatnagar et al., 1954). The discrete velocity is expressed as

$$\begin{aligned}
&\mathbf{e}_0 = (0, 0)\\
&\mathbf{e}_{1,3,5,7} = \left(cos\frac{(i-1)\pi}{4}, sin\frac{(i-1)\pi}{4}\right)\\
&\mathbf{e}_{2,4,6,8} = \sqrt{2}\left(cos\frac{(i-1)\pi}{4}, sin\frac{(i-1)\pi}{4}\right)
\end{aligned} \tag{2}$$

f_i^{eq} is an equilibrium distribution function, the choice of which determines the physics inherent in the simulation (Azwadi and Tanahashi, 2006).

In the free-energy two-phase lattice Boltzmann model, the equilibrium distribution determines the physics inherent in the simulation. A power series in the local velocity is assumed.

$$\begin{aligned}
&f_i^{eq} = A + B(e_{i,\alpha}u_\alpha) + C(e_{i,\alpha}e_{i,\beta}u_\alpha u_\beta) +\\
&Du^2 + G_{\alpha\beta}e_{i,\alpha}e_{i,\beta}
\end{aligned} \tag{3}$$

where the summation, over repeated Cartesion indices, is understood. The coefficients *A*, *B*, *C*, *D* and $G_{\alpha\beta}$ are determined by placing constraints on the moments of f_i^{eq}. The collision term conserves mass and momentum, and therefore the first moments of f_i^{eq} are constrained by

$$\sum_i f_i^{eq} = \rho \tag{4}$$

$$\sum_i e_{i,\alpha} f_i^{eq} = \rho u_\alpha \tag{5}$$

The continuum macroscopic equations approximated by the evolution equation correctly describe the hydrodynamics of a one-component, non-ideal fluid by choosing the next moment of f_i^{eq}. This gives

$$\begin{aligned}
&\sum_i e_{i,\alpha}e_{i,\beta}f_i^{eq} = P_{\alpha\beta} + \rho u_{\alpha\beta} +\\
&\upsilon\left[u_\alpha\partial_\beta(\rho) + u_\beta\partial_\alpha(\rho) + u_\gamma\partial_\gamma(\rho)\delta_{\alpha\beta}\right]
\end{aligned} \tag{6}$$

where $\upsilon = \left((\tau - 1/2)\Delta t\right)/3$ is the kinematic shear viscosity, $P_{\alpha\beta}$ is the pressure tensor, and τ is the time relaxation. In order to fully constrain the coefficients *A, B, C, D,* and $G_{\alpha\beta}$, a fourth condition is applied, which is

$$\sum_i e_{i,\alpha}e_{i,\beta}e_{i,\gamma}f_i^{eq} = \frac{\rho c^2}{3}\left(u_\alpha\partial_{\beta\gamma} + u_\beta\partial_{\alpha\gamma} + u_\gamma\partial_{\alpha\beta}\right) \tag{7}$$

The values of the coefficients can be determined by a Chapman-Enskog procedure. For the constraints (4)-(7), one possible choice of coefficients

$$\begin{aligned}
&A_1 = 2A_2,\ A_0 = \rho - 12A_2\\
&A_2 = \frac{P_o}{8c^2} + \frac{\upsilon}{4c^2}\left(u_x\partial_x\rho + u_y\partial_y\rho\right)\\
&B_2 = \frac{\rho}{12c^2},\ B_1 = 4B_2\\
&C_2 = \frac{\rho}{8c^4},\ C_1 = 4C_2\\
&D_2 = -\frac{\rho}{16c^2},\ D_1 = 2D_2,\ D_0 = 12D_2\\
&G_{2xx} = \frac{\kappa}{16c^4}\left[(\partial_x\rho)^2 - (\partial_y\rho)^2\right] +\\
&\frac{\upsilon}{8c^4}\left(u_x\partial_x\rho - u_y\partial_y\rho\right)\\
&G_{2xy} = G_{2yx} = \frac{\kappa}{8c^4}\left[(\partial_x\rho)(\partial_y\rho)\right] +\\
&\frac{\upsilon}{8c^4}\left(u_x\partial_x\rho - u_y\partial_y\rho\right)\\
&G_{2yy} = -G_{2xx}\\
&G_{1\alpha\beta} = 4G_{2\alpha\beta}
\end{aligned} \tag{8}$$

The analysis of Holdych et al. (2001) shows that the evolution scheme, Equation (1), approximates the continuity equations

$$\partial_t\rho + \partial_\alpha(\rho u_\alpha) = 0 \tag{9}$$

and the following Navier-Stokes equation

$$\begin{aligned}
&\partial_t(\rho u_\alpha) + \partial_\beta(\rho u_\alpha u_\beta) = -\partial_\beta P_{\alpha\beta} +\\
&\upsilon\partial_\beta\left[\rho\{\partial_\beta u_\alpha + \partial_\alpha u_\beta + \delta_{\alpha\beta}\partial_\gamma u_\gamma\}\right]
\end{aligned} \tag{10}$$

We have, then, described a framework for a one-component free energy lattice Boltzmann model. The theory of a Van Der Waals fluid is very close related to the multiphase phenomenon. The Van Der Waals state equation, can be written as

$$\left(\tilde{P} + \frac{3}{\tilde{V}^2}\right)(3\tilde{V} - 1) = 8\tilde{T} \tag{11}$$

where

$$\tilde{P} = \frac{P}{P_C}; \tilde{V} = \frac{V}{V_C}; \tilde{T} = \frac{T}{T_C}; V_C = 3b;$$
$$T_C = \frac{8a}{27bR}; P_C = \frac{8a}{27b^2} \quad (12)$$

and n is the mole number, a and b are constant characteristic of a particular gas and R is the gas constant. P, V and T are as usual the pressure, volume and absolute temperature, respectively.

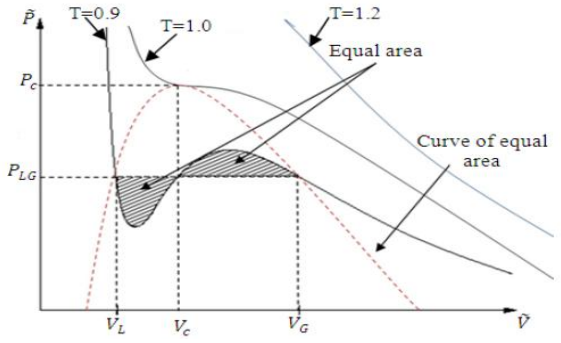

Figure 1 Isotherm plot of $\tilde{P}$-$\tilde{V}$

Figure 1 shows the plot of isotherm on a $\tilde{P} - \tilde{V}$ diagram for various $\tilde{T}$. For T greater than T_C, (~ is removed for simplification), the graph looks very much like the ideal gas isotherms. The system separates into two phases, a gas of volume V_G and a liquid volume V_L, when T less than T_C. The gas and liquid phases have the same pressure, P_{LG}. The value of V_G and V_L can be calculated by recalling the equilibrium condition, and the chemical potentials of the two phases must be equal. By using the Maxwell equal area construction, V_G and V_L can be determined. For example, for T = 0.55, the value of V_G, and V_L are 0.4523 (or density ρ_G = 2.221) and 0.2043 (or density ρ_L=4.895) respectively.

The thermodynamics of the fluid enters the lattice Boltzmann simulation via the pressure tensor. The equilibrium properties of a system with no surface (i.e periodic boundaries) can be described by a Landau free energy functional

$$\psi = \int dV \left[\psi(\rho, T) + \frac{\kappa}{2} (\partial_\alpha \rho)^2 \right] \quad (13)$$

subject to the constraint

$$M = \int dV \rho \quad (14)$$

where $\psi(\rho, T)$ is the free energy density of the bulk phase, κ is a constant related to the surface tension, M is the total mass of fluid and the integrations are over all space. The second term in Equation (13) gives the free energy contribution from density gradients in an inhomogeneous system. For a Van Der Waals fluid, the free energy density bulk phase can be written in the form

$$\psi(\rho, T) = \rho RT \ ln\left(\frac{\rho}{1 - b\rho}\right) - a\rho^2 \quad (15)$$

Introducing a constant Lagrange multiplier, μ, we can minimize Equation (15), giving a condition for equilibrium as

$$\frac{\partial \psi}{\partial \rho} - \mu - \kappa \nabla^2 \rho = 0 \quad (16)$$

By multiplying Equation (16) by $\partial\rho/\partial x$ and integrating once with respect to x, we obtain the first integral

$$\psi - \mu\rho - \frac{\kappa}{2} (\partial_\alpha \rho)^2 = \text{constant} \quad (17)$$

At the equilibrium condition, the chemical potential and pressure of both phases are given by

$$\mu = RT \ ln\left(\frac{\rho}{1 - b\rho}\right)\left(\frac{RT}{1 - b\rho}\right) - 2a\rho \quad (18)$$

$$p = \left(\frac{\rho RT}{1 - b\rho}\right) - a\rho^2 \quad (19)$$

respectively. We now define $W(\rho, T) = \varphi - \mu\rho + p$ meaning that Equation (18) and Equation (19) can be rewritten as

$$\frac{\partial W}{\partial \rho} = \kappa \nabla^2 \rho \quad (20)$$

and

$$W = \frac{\kappa}{2} (\partial_\alpha \rho)^2 \quad (21)$$

By solving Equation (21), we are able to determine the density profile at the interface for different values of κ, as shown in Figure 2. Fourth-order Rungge-Kutta is used to solve Equation (21), and the temperature is set at T = 0.55. As can be seen from the graph, the value of κ is related to the density gradient at the interface and affects the width of the interface.

3. NUMERICAL RESULTS

3.1 Phase Separation

In this section, the phase separation, which is based on the thermodynamic instability of the Van Der Waals fluid, is

simulated. If the initial state is set to an isothermally unstable region, according to the equation of state, the system will automatically separate into liquid and vapor phases and then achieve the equilibrium state.
The D2Q9 model with a 101 × 101 lattice was used, and the simulation was done at $T = 0.55$. Other parameters are presented in Table 1.

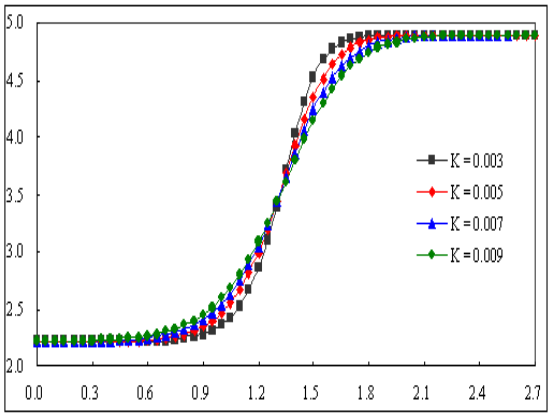

Figure 2 Density gradient at the interface

Table 1: Parameters used for the simulation of phase separation

Δx	Δy	Δt	τ	κ
1.0	1.0	1.0	1.00	0.0001

The transient behaviour of the phase separation was simulated in order to examine the validity of the model. Figure 3 shows the domain morphology at time steps of 2, 200, 500 and 20000 separately. Although the initial bubble nuclei are small, the mass densities inside the droplet are close to their equilibrium value. The small bubbles coalesce and form progressively larger bubbles over time. Consequently, a spherical bubble at the equilibrium state is formed. The interface during the system evolution is clear and retains same thickness. In Figure 3, the density contour distribution clearly describes the phase separation of the liquid and vapour. High density (blue) is the liquid phase and low density (red) is the vapour phase. At the equilibrium condition (20000 time steps), the initial bubble nuclei finally form a circular bubble to minimise the surface tension area.

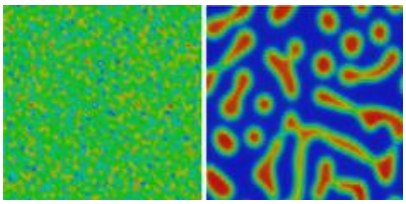

(a) 2 time steps (b) 200 time steps

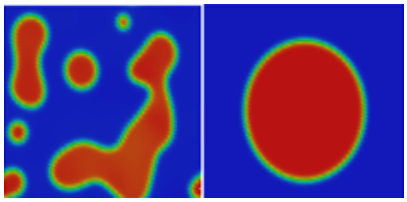

(c) 500 time steps (d) 2000 time steps

Figure 3 Snapshots of phase separation from 2 to 20000 time steps

3.2 Droplet spreading without gravitational effect

In this section, the droplet spreading phenomenon on a horizontal flat plate is simulated using the approach described in the preceding section. Initially, the droplet was set at a 180° contact angle or in non-wetting conditions. The droplet was then left to spread until it reached the equilibrium contact angle θ_w. Figure 4 shows the droplet on flat surface at various contact angles. In order to verify the simulated results, a graph of the ratio of the droplet wet length a_0 to the droplet height b_0 was plotted and compared with the analytical results given by Dullean et al. (1991) and shown in Figure 5.

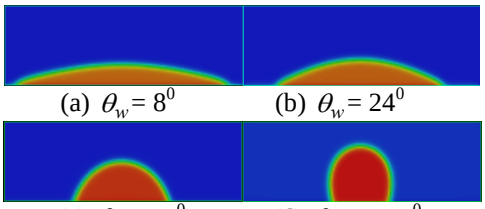

(a) $\theta_w = 8^0$ (b) $\theta_w = 24^0$

(c) $\theta_w = 70^0$ (d) $\theta_w = 104^0$

Figure 4 Droplet at various contact angles

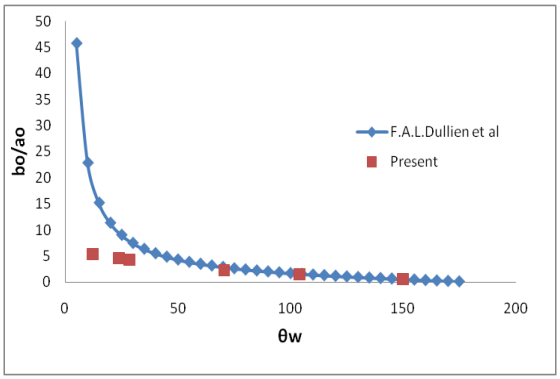

Figure 5 Comparison of results for the ratio of droplet wet length to droplet height at various droplet contact angles

Results of the comparison in Figure 5 clearly show that the droplet contact angle is in good agreement with theoretical value when the contact angle is larger than 70° or in a partial wetting condition to non-wetting. However, when the contact angle is lower than 70^0, the computational results

show some disagreement with the theoretical value. This problem will be studied in our future research. In the next section, the deformation of the droplet under a gravitational force on a horizontal plate will be discussed.

3.3 Droplet Spreading with Gravitational Effect

The effect of the gravitational force plays a vital role in determining the shape of a droplet for several of Bond numbers. The dimensionless Bond number reflects the balance between the gravitational and capillary forces, given by

$$Bo = \frac{r^2 \rho g}{\sigma} \qquad \textbf{(22)}$$

In our simulation, we varied the value of gravitational force g, to obtain various values of the Bond number. Then the simulated droplets at the equilibrium condition were compared quantitatively with those of Murakami et al. (1998) (not shown).

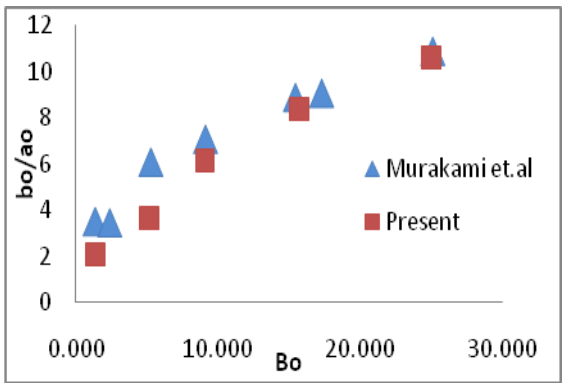

Figure 6 Comparison of results for the ratio of the droplet wet length and droplet height at various Bond numbers

The ratio of droplet wet length and droplet height is again plotted with the Bond number. The comparison of results between the present approach and the experimental data by Murakami et al. is presented in Figure 6. Good agreement can be seen between these two approaches.

3.4 Droplet Falling

In this section, the results for a droplet falling are presented. The initial droplet contact angle at the ceiling plane is set to 90^0, which is the same initial condition as used by Ozawa et al. (2005). The present result shows that the droplet starts to separate from the ceiling at the 15000 time step, where this is in quantitatively good agreement with the simulation results of Ozawa et al.

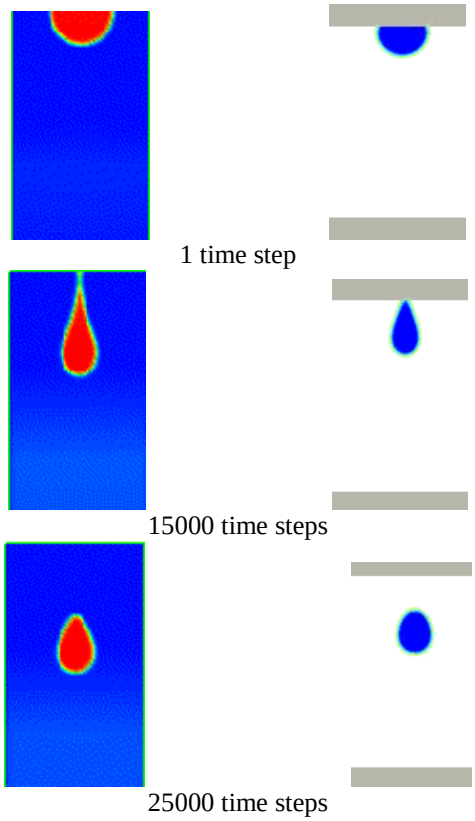

Figure 7 Droplet falling from flat top wall (left: present simulation results, right: Simulation results from Ozawa et al.

4. CONCLUSION

This paper has shown the capabilities of the lattice Boltzmann method in solving the two-phase system. The advantages of the multiphase lattice Boltzmann approach are not only the capability of incorporating interface deformation and interaction but also the interparticle interactions, which are difficult to implement in tradiational methods. The two phase-flow benchmark test showed the relaxation process of the droplet, which is in agreement with the results of other researchers. It is demonstrated that the free energy two-phase lattice Boltzmann model has the capability to simulate phase separation, droplet spreading and droplet falling phenomena. The phase separation has been correctly predicted where the value of density for both phases at the equilibrium state are in good agreement with the isothermal P-V graph. The numerical results of the droplet spreading and falling indicate that the two-phase lattice Boltzmann scheme may be applicable for simulating interfacial dynamics in immiscible phases.

REFERENCES

Azwadi, C. S., Idris, M. S., 2010. Finite difference and lattice Boltzmann modeling for simulation of natural convection in a square cavity, International Journal of Mechanical and Materials Engineering, 5 (1), 80-88.

Azwadi, C. S., Tanahashi, T., 2006. Simplified termal lattice Boltzmann in incomprensible limit, International Journal of Modern Physics B, World Scientific, 20, 2437-2449.

Azwadi, C. S., Tanahashi, T., 2007. Mulltiphase flow simulation with lattice Boltzmann method, Jurnal Mekanikal, Universiti Teknologi Malaysia, Malaysia, 24, 68-79.

Bhatnagar, P. L., Gross, E. P., Krook, M., 1954. A model for collision process in gasses, Physical Review, America Physical Society, America, 94 (3), 511-525.

Briant, A. J., Papatzacos, P., Yeomans, J. M., 2002. Lattice Boltzmann simulations of contact line motion in a liquid–gas system, Philosophy Transaction Royal Society London A, Royal Society, UK , 360, 485–495.

Dullean, F. A. L., 1979. Porous Media: Fluid Transport and Pore Structure, Academic Press.

Gunstensen, A.K., Rothman, D. H., Zaleski, S., Zanetti, G., 1991. Lattice Boltzmann model of immiscible fluids, Physical Review A, American Physical Society, 43(8), 4320–4327.

Hasanuzzaman, M., Saidur, R. and Masjuki, H. H. Effects of operating variables on heat transfer, energy losses and energy consumption of household refrigerator-freezer during the closed door operation, Energy, 34(2), 2009, 196-198.

Hasanuzzaman**,** M., Saidur, R., Ali, M. and Masjuki, H.H. Effects of variables on natural convective heat transfer through V-corrugated vertical plates**,** International Journal of Mechanical and Materials Engineering, 2(2), 2007, 109-117

Holdych, D. J., Geogiadis, J. G., Buckius, R. O., 2001. Migration of a Van-Der Waals bubbles: Lattice Boltzmann formulation, Physics of Fluid, American Institute of Physics, 13, 817-825.

Murakami, K., Nomura, S., Shinozuka, M., 1998. Numerical analysis of shape of liquid droplet on solid surface with SOLAVOF method, Japanese Journal of Multiphase Flow, The Japan Society of Multiphase flow, 12, 56-58.

Ozawa, T., 2006. Fluid flow simulation using unstructured lattice Boltzmann formulation, Keio University, Japan.

Rothman, D. H., Keller, J. M., 1988. Immiscible cellular-automaton fluids, Journal of statistical physical, 52, 1119-1127.

Shan, X., Chen, H., 1993. Lattice Boltzmann model for simulating flows with multiple phases and components, Physical Review E, American Physical Society, 47 (3) 1815-1820.

Swift, M. R., Osborn, W. R., Yeoman, J. M., 1995. Lattice Boltzmann simulation of non-ideal fluids, Physical Review Letters, American Physical Society, 57 (5), 830-833.